STARS

Retrospective Theses and Dissertations

1995

Gaussian beam resonator formalism using the yy method

Kenneth A. Menard
kenmenard1983@yahoo.com

University of Central Florida

STARS
Showcase of Text, Archives, Research & Scholarship

GAUSSIAN BEAM RESONATOR FORMALISM USING THE $y\bar{y}$ METHOD

by

KENNETH A. MENARD
B.Sc., University of Waterloo, 1983
M.A.Sc., University of Toronto, 1986

THESIS

Submitted in partial fulfillment of the requirements
for the degree of
Masters of Science in Electrical Engineering
Department of Electrical Engineering
College of Engineering
University of Central Florida
Orlando, Florida

Summer Term
©1995

ABSTRACT

A simple and powerful new paraxial ray formalism is shown to provide an alternate method for designing Gaussian Beam Resonators. The theory utilizes the Delano or yybar diagram approach and is an extension of the recent work by Shack and Kessler for laser systems. The method is shown to be complementary to the conventional ABCD method and is founded upon J.A. Arnaud's pioneering ideas for complex rays.

The thesis develops an analytic formulation of a ray based complex wavefront curvature and yields a clearly generalized description of spherical wave propagation, for which Gaussian beams are considered a special case. The resultant theory unifies the complex q parameter and the ABCD law, with the yybar complex ray components and also suggests that the ABCD law for the complex q parameter has its origin in the yybar complex ray.

New fundamental equations for designing stable multi-element resonators using the yybar coordinates are derived, and it is shown that the yybar diagram provides a novel method for defining automatically stable resonators. Various applications for the yybar design technique are also discussed, including the setting of convenient design constraints, the description of M^2 beams, generating phase diagrams, and resonator synthesis and analysis.

ACKNOWLEDGMENTS

TABLE OF CONTENTS

LIST OF TABLES

LIST OF FIGURES

CHAPTER 1

INTRODUCTION

"There are new and exciting problems arising that are a combination of traditional lens design and new device-oriented photonics applications. In many of these new problems, the geometrical model is not adequate, nor is a beam propagation model adequate on its own. Integrating these design tools and developing the understanding of how to use them are still in their early stages.

The recent meeting of the lens designer and the photonics physicist was a start toward development of this field. Those who fail to work toward a union of these optical opportunities will likely be left behind."

R. R. Shannon, 1993 [1.1]

The field of laser engineering has continually evolved since the invention of the laser in 1960, both with regard to technological advances, as well as to theoretical models. In particular, the Gaussian beam model of a laser resonator has achieved tremendous attention in this field, mainly because of its great effectiveness as a tool for predicting beam behavior.

Various techniques of implementing the Gaussian model to solve beam propagation and resonator problems, have also evolved. In the mid 1960s, H. Kogelnik of Bell Telephone Laboratories developed what is now termed the ABCD method of solution [1.2]. While its matrix formulation is well suited to computer calculation, it's 'ABCD Law' is also convenient for algebraically predicting resonator stability, beam size and radius of curvature at a chosen plane, given the mirror radii and the distance between

them. The method is now practically exclusive and is typically the foundation of virtually all text books on laser theory.

The purpose of this work is to introduce a new and alternate paraxial ray technique, termed the $y\bar{y}$ (pronounced and hereafter called, the 'yybar') method, for solving Gaussian beam resonator problems. The theory is based on J. A. Arnaud's pioneering ideas for complex rays [1.3,1.4], and is an extension of the powerful yybar formalism recently presented by Kessler and Shack for laser beam propagation [1.5, 1.6]. The thesis will develop an analytic formulation of a ray based complex wavefront curvature and yield a clearly generalized description of spherical wave propagation, for which Gaussian beams are considered a special case. The connection between the complex q parameter, the ABCD law, and the yybar complex ray components will also be explored, and then we will depart from the traditional ABCD 'eigenvalue' method, concentrating instead on confining a special pair of rays within an optical resonator.

New fundamental equations for designing stable multi-element resonators using the yybar coordinates will be derived, and it will be shown that the yybar diagram (also referred to as the Delano diagram) provides a novel method for defining automatically stable resonators. It will also be shown that this new method is complementary to the ABCD technique, and that it is capable of yielding complete ABCD component information, given the desired ray trace of the cavity, and yielding a complete ray trace, given the ABCD component information. The formalism will also demonstrate that the

yybar technique allows one to conveniently synthesize and analyze complicated multi-element resonator designs, while constraining each design to be automatically stable.

The work begins with a brief history of the general yybar diagram and reviews some previous theory related to the application of yybar principles to Gaussian laser beams. After a review of the conventional resonator ray description, the second chapter then introduces the concept of a complex yybar ray, based on Arnaud's formulations, and shows how it is linked to the complex q parameter for Gaussian beams. Since the ABCD law is now the most familiar and conventional method of designing laser resonators, chapter two goes on to show that its origin is effectively found in complex ray formalism. The chapter also discusses the important (but historically reversed) link between the ABCD method and the classic ray trace formalism, on which the yybar method is based.

Chapter three begins with a brief outline of yybar diagram principles, ideas, and method of construction, and then introduces the main concepts and formalism required to define yybar laser resonators. The resonator stability conditions are then derived in terms of yybar variables, and then the collection of common two mirror resonators are mapped onto the yybar plane. The methods are then extended to more complicated resonators, those having multiple internal optical components.

In chapter four, some applications for the yybar method are discussed, including the setting of convenient design constraints, the design of M^2 beam resonators, the use of the yybar diagram as a phase diagram, beam size analysis (given the ABCD matrices), and

the synthesizing of resonators. The work concludes with a summary and some

recommendations for future research of this invaluable new tool.

1.1   <u>**Brief History of the General yybar Diagram**</u>

In 1963, E. Delano introduced a new method for graphically determining the

first-order layout of an arbitrary "...optical system of axially symmetric refracting or

reflecting surfaces" [1.7]. Rather than using the properties of the optical elements as the

defining parameters of an optical system, his yybar diagram method chose the height of the

marginal ray (y), the height of the chief ray (ybar), the Lagrange invariant (H), and a pair

of object and image reference planes. The next year, R. J. Pegas demonstrated a

numerical yybar method for "Semiautomatic Generation of Optical Prototypes" [1.8].

Given first order constraints, a yybar diagram was automatically generated and optimized

for the lowest speed. The ray angle (u and ubar) information was then used while varying

the individual surface properties to minimize third order Seidel aberrations.

In 1970, F. J. López-López introduced a normalization process, y by the entrance

pupil height, and ybar by the image height [1.9]. This allowed the additional constraints of

system focal length, numerical aperture, and field aperture to be easily applied, while

varying any number of refractions and transfers. Several years later, Roland Shack

popularized the yybar diagram further with practical examples and also provided new

insight into its elegance, utility, and power [1.11]. At the same time, F. J. López-López

developed additional analytical tools for analyzing and synthesizing system properties,

using vector geometry [1.10]. Other contributions include the work of Walter

Besenmatter pertaining to zoom lens design [1.12], and the GRIN design applications of

Harrigan, Loce, and Rogers [1.13, 1.14].

In addition to using the yybar diagram as an optical design tool, the use of yybar

variables on their own, provides a powerful method of optical design, when used with the

optical invariant condition. This is demonstrated, for example, by P. Trotta [1.15].

1.2 Previous Related Theory Applied to Gaussian Laser Beams

In 1969, J. A. Arnaud [1.3-1.5] attached physical significance to Kogelnik's

complex paraxial definition, q=X/(dX/dz), for Gaussian beam propagation [1.2], by

showing that the imaginary and real components of the complex ray, represent real rays

which are directly related to the beam size and beam radius. He also recognized that the

components could be used to form a real skew ray and that the projection of the

components formed an interesting phase diagram. Although equivalent to a yybar

diagram, it was not recognized as one.

In 1983, Herloski et al used Arnaud's theory to define a waist ray height (y_1) and a

divergence ray height (y_2) to define Gaussian beam propagation through a conventional

ABCD matrix system [1.16]. Using Code V and the relationship, $\omega^2 = y_1^2 + y_2^2$, the beam

size could be set as a numerical constraint, or tracked through the system. In 1984 and

1992, D. Kessler and R. V. Shack formally showed that the two Gaussian beam paraxial

rays could be represented on a yybar diagram, resulting in a new method for analyzing and

synthesizing complicated laser beam optical systems [1.5,1.6]. The use of strictly yybar

variables (without the yybar diagram), together with the Lagrange Invariant condition, has

also become recently popular for describing Gaussian laser beams [1.17]. Apparently,

none of the previous work has applied yybar formalism to (laser type) resonator design.

CHAPTER 2

RELATING THE COMPLEX RAY TO THE GAUSSIAN COMPLEX RADIUS AND THE ABCD METHOD

2.1   A Review of Conventional Resonator Ray Description

Let us review the conventional ABCD method of confining rays within a cavity.

First, consider the displacement, r_n of an arbitrary ray in an optical medium. In

conventional ABCD matrix form, we have,

$$\begin{bmatrix} r_n \\ r_n' \end{bmatrix} = \begin{bmatrix} A & B \\ C & D \end{bmatrix} \begin{bmatrix} r_{n-1} \\ r_{n-1}' \end{bmatrix} \tag{2.1}$$

where the matrix elements, A, B, C, and D, are the ray coefficients, usually for a

compound system of elements. This 'bundle' of arbitrary rays is shown to have an

oscillation solution when confined to a cavity like structure. The solution has the form

(see, for example, Siegman [2.1], Yariv [2.5], or Verdeyen [2.6]):

$$r_n = r_0 \cos \theta n + s_0 \sin \theta n \tag{2.2}$$

where n is the number of sections, r_0 and s_0 are the initial ray properties, and the

condition, $-1 \le \cos \theta \le 1$, is found to be necessary for a stable solution, where

$\cos \theta = (A + D)/2$. The so-called eigenvalues are given by: $\lambda_1, \lambda_2 = \exp \pm j\theta$.

Ordinarily, this is the entire scope of ray displacement theory and analysis for the ABCD method of solution for resonators; any other quantitative information on beam size and location is usually derived in terms of the A, B, C, and D coefficients, not in terms of the ray or 'eigenray' quantities. In <u>this</u> work, it is normally the desired <u>ray</u> properties that are made convenient to choose, with the consequence that the coefficient values are determined secondarily, simply as a result of this choice, and as a matter of convenience.

2.2   **Arnaud's Complex Rays**

Consider an 'Arnaud' ray which is complex valued, such that both its real and imaginary components represent real rays. Such a ray could be defined in terms of the standard r and r' nomenclature, as follows:

$$\mathbf{r} = r_a + i r_b \qquad \text{and} \qquad \mathbf{r}' = r_a' + i r_b' \qquad (2.3)$$

However, it is convenient at this time to define a special ray, $\mathbf{Y}$, which we will call the yybar complex ray, and which has as its real and imaginary components, the two <u>real</u> y and ybar rays respectively. Its unique property will be defined later when we apply a strategic and convenient magnitude for it. For now, let us simply define it:

$$\mathbf{Y} = y + i\bar{y} \qquad \text{and} \qquad \mathbf{U} = u + i\bar{u} = d\mathbf{Y}/dz \qquad (2.4)$$

2.3   ABCD Law for Complex Rays

Since the standard ray transfer equations apply to both the complex and real

components of this special complex ray, they also apply to the complete ray:

$$\mathbf{Y}_2 = A\mathbf{Y}_1 + B\mathbf{U}_1 = A(y_1 + i\bar{y}_1) + B(u_1 + \bar{u}_1) \qquad (2.5)$$

and,

$$\mathbf{U}_2 = C\mathbf{Y}_1 + D\mathbf{U}_1 = C(y_1 + i\bar{y}_1) + D(u_1 + \bar{u}_1) \qquad (2.6)$$

Here, A,B,C and D are the conventional (real valued) matrix ray coefficients, for the

optical element or system between position 1 and 2. By dividing the two equations, we

arrive at a general form of the familiar ABCD law, in this case for complex rays:

$$\mathbf{Y}_2/\mathbf{U}_2 = (y_2 + i\bar{y}_2)/(u_2 + i\bar{u}_2) = (A\mathbf{Y}_1/\mathbf{U}_1 + B)/(C\mathbf{Y}_1/\mathbf{U}_1 + D) \qquad (2.7)$$

Also, the complex paraxial angle, **U**, is related to a complex radius of curvature, **R**, by the

subtending geometric expression,

$$\mathbf{U} = \mathbf{Y}/\mathbf{R} \qquad (2.8)$$

With this definition, we can see that the complex paraxial radius has a very basic

interpretation: it simply represents the complex distance which the wavefront has

propagated from its (complex) source. By direct substitution, we obtain,

$$\mathbf{R}_2 = (A\mathbf{R}_1 + B)/(C\mathbf{R}_1 + D) \qquad (2.9)$$

2.4   Relating the Complex Ray Radius to the Complex q Parameter

The real radius of curvature for the wavefront defined by this complex ray is

obtained by splitting the last equation into its real and imaginary parts. This can be done in

two ways. First, we solve for the inverse of $\mathbf{R}$:

$$1/\mathbf{R} = \mathbf{U}/\mathbf{Y} = (u + i\bar{u})/(y + i\bar{y}) = (\bar{u}\bar{y} + uy)/(y^2 + \bar{y}^2) + i(y\bar{u} - u\bar{y})/(y^2 + \bar{y}^2) \qquad (2.10)$$

The inverse of the real part of this expression is the wavefront radius,

$$R = (y^2 + \bar{y}^2)/(\bar{u}\bar{y} + uy) \qquad (2.11)$$

Now recognizing that H= $u\bar{y} - y\bar{u}$ is the Lagrange invariant, the expression for 1/$\mathbf{R}$ can be

re-written as,

$$1/\mathbf{R} = 1/R + iH/(y^2 + \bar{y}^2) \qquad (2.12)$$

Let us also solve for $\mathbf{R}$ directly:

$$\mathbf{R} = (y + i\bar{y})/(u + i\bar{u}) = (\bar{u}\bar{y} + uy)/(u^2 + \bar{u}^2) + iH/(u^2 + \bar{u}^2) \qquad (2.13)$$

These last two expressions are derived purely from paraxial ray principals. They are

completely general, and thus can be applied to any type of spherical wave propagation.

Both equations allow one to determine both the radius of the wavefront and its phase

properties. The second equation has the explicit form to determine how far the wavefront

has propagated from its complex source point.

Consider now the special case of an unaberrated, untruncated, and symmetric Gaussian beam, having radius, ω, at a chosen z plane. In this case, the effective complex radius of curvature is given by the well known expressions,

$$1/q = 1/R - i\lambda/\pi\omega^2 \qquad \text{and} \qquad q = q_0 + z = i\pi\omega_0^2/\lambda + z \qquad (2.14)$$

by comparison to the previous two equations, we can see that TEM_{00} Gaussian beam propagation can be considered as just a particular case of our general complex beam radius formulation.

Therefore, if we wish to constrain our y and ybar rays to describe Gaussian beam propagation, we simply equate the two complex radii, $q=R=Y/U$, to give:

$$H = u\bar{y} - y\bar{u} = \lambda/\pi \qquad\qquad \omega^2 = y^2 + \bar{y}^2 \qquad (2.15)$$

$$z = (\bar{u}\bar{y} + uy)/(u^2 + \bar{u}^2) \qquad\qquad \omega_0^2 = H^2/(u_0^2 + \bar{u}_0^2) \qquad (2.16)$$

We immediately arrive at four very important transformation relationships. The first two equations were derived previously by Arnaud, while the last two were recently derived with a geometric method by Kessler and Shack. Collectively, these definitions allow us to state a general ABCD law of transformation:

$$\mathbf{Y}_2/\mathbf{U}_2 = (y_2 + i\bar{y}_2)/(u_2 + i\bar{u}_2) = q_2 = (\mathbf{AY}_1/\mathbf{U}_1 + B)/(\mathbf{CY}_1/\mathbf{U}_1 + D) = (Aq_1 + B)/(Cq_1 + D)$$

$$(2.17)$$

Thus, for Gaussian beams, there is a simple relationship between the yybar variables, the complex q parameter, and the ABCD law of transformation. In fact, this expression shows the origin and conveniently proves the general validity of the ABCD law for the q parameter (at least for the presently assumed case of real valued A,B,C, and D coefficients). According to Verdeyen, it is generally considered "very difficult" to prove the ABCD law for the q parameter by common formalism (except through the methods of comparison and verification).

The reader is reminded here that this ABCD law, when combined with the so-called 'self-consistency condition', $q_2 = q_1$, is the central equation utilized in conventional resonator design. It is used to force the wavefront radius and the beam size to equal themselves at a single chosen plan after a round trip (characterized by the round trip system coefficients, A,B,C, and D). Although one could apply this same law to the yybar complex radius, and presumably determine equivalent information at the chosen plane, we shall find a far more fruitful method can be found for characterizing the resonator, at all planes. First, we need to expand on the topic of resonator ray tracing.

2.5   Converting the ABCD Matrices to Ray Trace Variables

To broaden the scope of conventional resonator ray analysis, we begin by relating the ABCD information to standard ray trace variables. Although the A,B,C, and D coefficients normally represent the compound effects of multiple optical elements (i.e. representing the total system matrix), let us consider the individual component matrices,

imposing for our purposes, that each matrix represents the effects of a single optical element, situated just in front of the incoming rays from the previous element.

Instead of an arbitrary ray 'bundle' set, {r}, let us select the two very <u>special</u> y, and ybar 'beam' rays, which are constrained to obey strict and chosen conditions. While both the y and ybar rays, and their respective propagation derivatives, u and ubar, conform to the conventional matrix format above (they are, of course, members of the general 'r' ray bundle defined previously), we shall write them out in the explicit ray trace format:

$$y_n = Ay_{n-1} + Bu_{n-1,n} \qquad \bar{y}_n = A\bar{y}_{n-1} + B\bar{u}_{n-1,n} \qquad (2.18)$$

$$u_{n,n+1} = Cy_n + Du_{n-1,n} \qquad \bar{u}_{n,n+1} = C\bar{y}_n + D\bar{u}_{n-1,n} \qquad (2.19)$$

In order that these ABCD coefficients conform to the Lagrange or 'Optical' invariant condition, we require,

$$H = y_{n+1}\bar{u}_{n+1,n+2} - u_{n+1,n+2}\bar{y}_{n+1} = y_n\bar{u}_{n,n+1} - u_{n,n+1}\bar{y}_n \qquad (2.20)$$

and by substitution,

$$y_{n+1}\bar{u}_{n+1,n+2} - u_{n+1,n+2}\bar{y}_{n+1} =$$

$$(Ay_n + Bu_{n,n+1})(C\bar{y}_n + D\bar{u}_{n,n+1}) - (Cy_n + Du_{n,n+1})(A\bar{y}_n + B\bar{u}_{n,n+1})$$

$$= (AD - BC)(y_n\bar{u}_{n,n+1} - u_{n,n+1}\bar{y}_n) \qquad (2.21)$$

Therefore, AD - BC = 1 is a necessary condition for using the coefficients. Since many optical components used in resonators have already been characterized in terms of ABCD matrix coefficients which meet this condition, these equations can assist us in determining the yybar paraxial representation of matrix elements.

In most cases, the value of the A and B coefficients is unity; but there are exceptions: for example, in GRIN type media, the A and B coefficients have sinusoidal arguments [2.5], and then this simplification cannot be made. Keeping this in mind, but assuming the values are unity, then,

$$y_n = y_{n-1} + Bu_{n-1,n} \qquad\qquad u_{n,n+1} = Cy_n + u_{n-1,n} \qquad\qquad (2.22)$$

$$\bar{y}_n = \bar{y}_{n-1} + B\bar{u}_{n-1,n} \qquad\qquad \bar{u}_{n,n+1} = C\bar{y}_n + \bar{u}_{n-1,n} \qquad\qquad (2.23)$$

By inspection, we find that the B coefficient represents the (reduced) distance between the n, n-1 planes, and -C represents the optical power of the element located at plane n. To match ray trace convention, we replace the symbols B, and -C with the τ, and ϕ respectively, to give:

$$\bar{y}_n = \bar{y}_{n-1} + \tau_{n-1,n}\bar{u}_{n-1,n} \qquad\qquad u_{n,n+1} = u_{n-1,n} - \phi_{n-1,n,n+1}y_n \qquad\qquad (2.24)$$

$$y_n = y_{n-1} + \tau_{n-1,n}u_{n-1,n} \qquad\qquad \bar{u}_{n,n+1} = \bar{u}_{n-1,n} - \phi_{n-1,n,n+1}\bar{y}_n \qquad\qquad (2.25)$$

CHAPTER 3

FORMALISM FOR THE yybar RESONATOR DESIGN

3.1   Basic YYbar Diagram Principles

While the yybar diagram method is generally applicable to any image based optical

system, the basic technique has not achieved as much popularity as it deserves.

Unfamiliar readers are strongly urged to thoroughly read the previously cited references,

especially the heavily referenced paper by Kessler and Shack [1.6]. What follows is an

extremely brief review, for the strict purpose of introducing only the needed central

concepts.

Let us first consider a basic (two dimensional) single lens image system. After

tracing two merdional rays (choosing the marginal and chief rays), one can plot the two

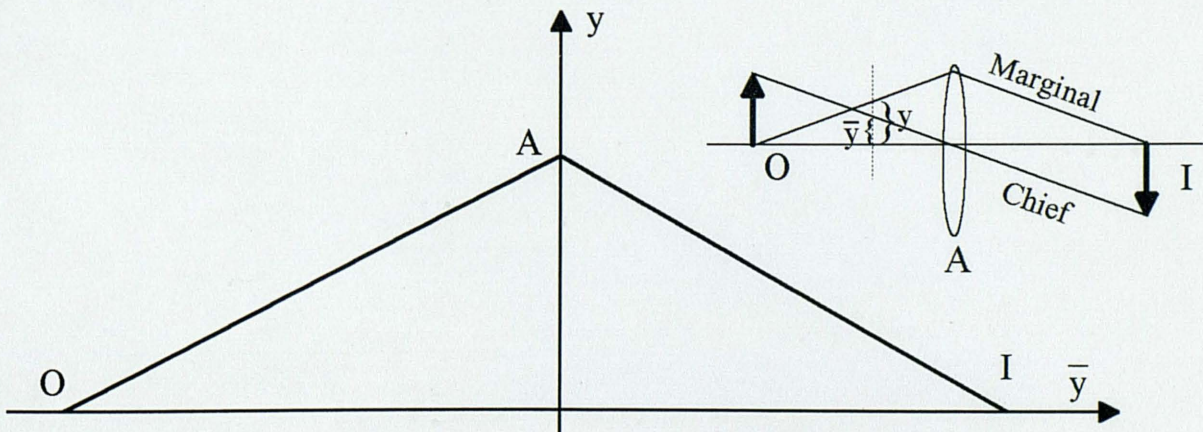ray displacements as the abscissa and ordinates on what is termed a yybar diagram, as

shown below:

Figure 3.1: yybar Diagram for Single Lens Imaging

At its most basic level, the yybar diagram provides a simple and effective method for generating and analyzing an optical system by tracing through any two different rays. In the previous work of Delano and Shack, the concept is reduced further to a single skew ray trace which has as its orthogonal components a marginal and a chief ray. Although Arnaud (independent of Delano's work) also originated a skew ray "generator" for Gaussian beams, we will avoid its use.

Instead, we will choose to use the yybar coordinate information directly, and associate the y and ybar values with what Kessler and Shack refer to as the y and ybar rays, respectively. (This is also what was done, effectively, by Herloski et al [1.16]). With the two rays defined in this manner, they become equivalent to the y and ybar rays we discussed in Chapter 2; and, in particular, they can represent the Gaussian beam rays we derived earlier--namely as real and imaginary components of the complex **Y** ray, which are constrained to define the magnitude of the beam size. With this y and ybar ray representation, we shall find that the Gaussian beam resonator is easily defined.

Reducing the skew ray condition not only offers further simplicity for defining Gaussian beam yybar formalism, it also removes Delano's axially symmetric requirement, thus allowing the two yybar rays to lie in a <u>meridional</u> plane. As Herloski et al recognized, this also allowed their yybar-like variables to be used for simply astigmatic systems. (These simplifications can also be applied to image based systems).

Even with the changes we have made to suit our Gaussian beam formalism, most of the yybar concepts still apply. They include:

(1) Area on the diagram represents distance.

(2) Points represent planes.

(3) Any straight line passing through the origin represents a conjugate line, with object and image planes defined by the ray trace intersections.

(4) The y and ybar axis represent conjugate lines.

3.1.1 Equations Required for Computation

The yybar variables themselves can be used to supplement the diagram with analytical formulations. Let us now summarize the key equations required for an analytical determination of the yybar trace in the customary manner:

Refraction: $\quad u_{23} = u_{12} - y_2 \phi_{123}$, $\qquad\qquad \bar{u}_{23} = \bar{u}_{12} - \bar{y}_2 \phi_{123}$ $\qquad\qquad$ (3.1)

Transfer: $\quad y_2 = y_1 + \tau_{12} u_{12}$, $\qquad\qquad \bar{y}_2 = \bar{y}_1 + \tau_{12} \bar{u}_{12}$ $\qquad\qquad$ (3.2)

Lagrange Invariant: $\quad H = y_i \bar{u}_{i,i+1} - \bar{y}_i u_{i,i+1}; i = 1..n$ $\qquad\qquad$ (3.3)

Distance: $\quad \tau_{12} = (y_1 \bar{y}_2 - y_2 \bar{y}_1)/H$ $\qquad$ Power: $\quad \phi_{123} = (u_{12} \bar{u}_{23} - u_{23} \bar{u}_{12})/H$ $\qquad$ (3.4)

As Delano has shown, the last two equations are derived by substituting the Transfer and Refraction equations into the Lagrange Invariant relation, respectively.

3.1.2 Constructing YYbar Tables

We now wish to determine the required focal length of the lens system in the yybar diagram of figure 3.1. It is convenient to determine the unknown lens power by using the table filling technique shown below [1.11]:

Table 3.1: yybar Table for a Single Imaging Lens System

y	$\bar{y}$	τ	u	u	ϕ
y_1	0				
		τ_{12}	$(y_2 - y_1)/\tau_{12}$	$(\bar{y}_2 - \bar{y}_1)/\tau_{12}$	
y_2	$\bar{y}_2$				$\bar{y}_2(y_1 - y_2)/H\tau_{12}\tau_{23}$
		τ_{23}	$(y_3 - y_2)/\tau_{23}$	$(\bar{y}_3 - \bar{y}_2)/\tau_{23}$	
y_3	0				

Since,

$$\tau_{12} = y_1\bar{y}_2/H \quad \text{and} \quad \tau_{23} = -y_3\bar{y}_2/H \tag{3.5}$$

then,

$$\phi = (\tau_{12} + \tau_{23})/\tau_{12}\tau_{23} \tag{3.6}$$

which yields the imaging law,

$$\frac{1}{f} = \frac{1}{\tau_{12}} + \frac{1}{\tau_{23}} \tag{3.7}$$

This ends the brief outline of the basic yybar diagram principles, and we are now at a point where we can define an optical resonator with yybar formalism.

3.2   Defining the yybar Resonator Geometry

Consider any two arbitrary points, $(\bar{y}_1, y_1)$ and $(\bar{y}_2, y_2)$ on the yybar diagram. Without any loss of generality, we can represent the two points such that the line from the origin perpendicular to the segment which joins them, lies along the positive y axis (refer to figure 3.2 below):
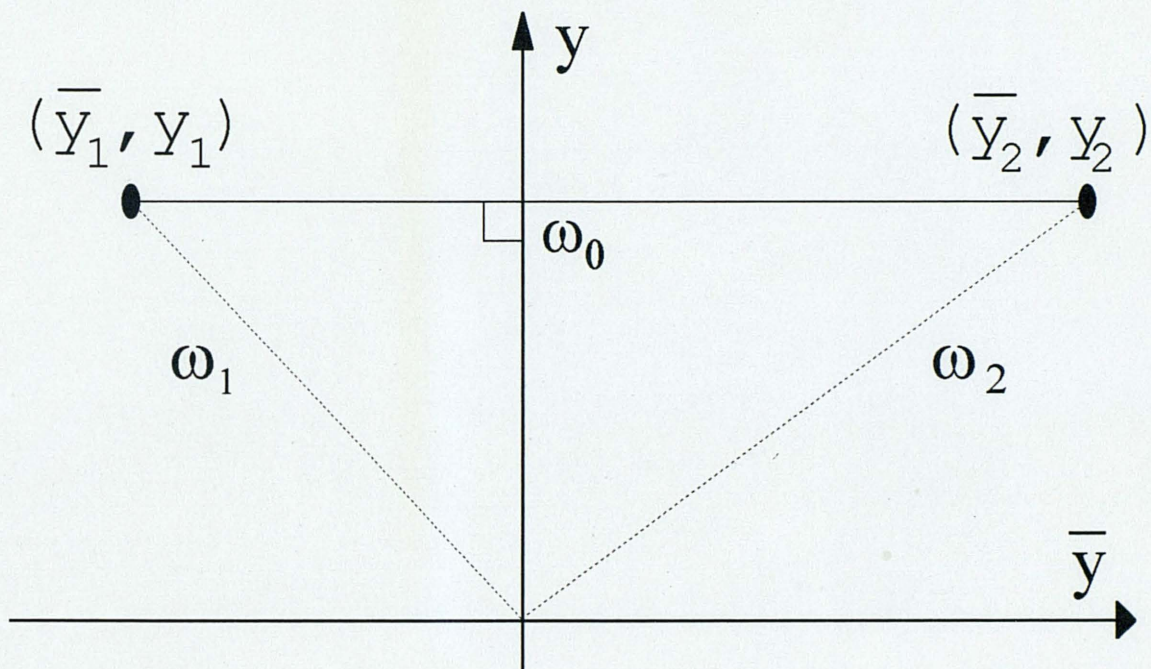
Figure 3.2: Simple yybar Diagram Describing Gaussian Beam Propagation Between Two Arbitrary Points.

Note the reason there is no loss in generality for this choice of configuration is because coordinate rotation about the origin is allowed, since all points retain their respective spacing with respect to the origin. A rotation with our formalism can be interpreted as choosing an equivalent, but different, pair of paraxial y and ybar paraxial rays [1.7].

By definition, the line joining the two points represents the propagation of a

Gaussian wavefront. The diagram depicts area as the distance the beam propagates,

normals terminating at the origin as beam waists, and the angle between points as the

phase of the wavefront. The beam size, ω, is represented by the distance from the origin

to the trace, and can be determined at any plane along the path of the beam. In figure 3.2

the beam size is indicated at the two end points; however, it can easily be defined at any

other point along the trace. The beam waist is indicated along the y axis and occurs there

only because we have chosen the beam trace to be perpendicular to that axis.

If we 'confine' the beam by placing two mirrors at these coordinates with radii

determined from, $R = (y^2 + \bar{y}^2)/(\overline{uy} + uy)$, then the Gaussian radiation is continually

re-mapped, or reflected in between the two points. Since the mirror radii exactly matched

the wave front radii, the resultant 'resonance' is automatically stable, and all radiation is

thus constrained to remain within this fundamentally defined resonator (see figure 3.3).
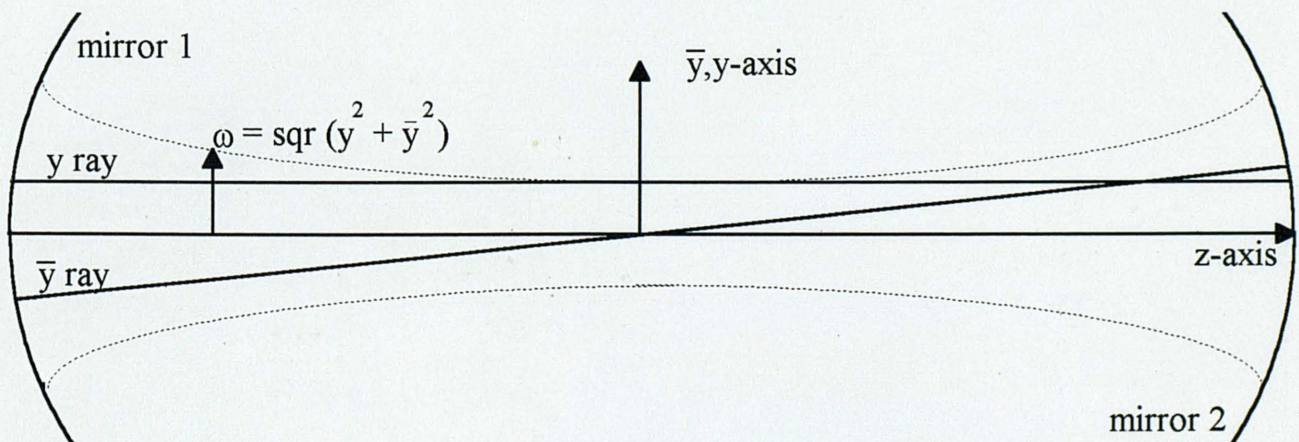
Figure 3.3: Gaussian Beam Resonator Showing the Defining y and ybar Rays.

3.3 Resonator Length, Mode Volume, and Confocal Parameter

The resonator is characterized by mirror spot sizes, ω_1, ω_2 and intra-cavity beam waist, ω_0, and by cavity length,

$$L \equiv (y_1\bar{y}_2 - y_2\bar{y}_1)/H \tag{3.8}$$

The beam waist can be expressed as,

$$\omega_0 = (y_0^2 + \bar{y}_0^2)^{1/2} = H/(u_0^2 + \bar{u}_0^2)^{1/2} \tag{3.9}$$

The mode volume within the resonator is [2.6]:

$$V_m = \omega_0^2 L = (y_0^2 + \bar{y}_0^2)(y_1\bar{y}_2 - y_2\bar{y}_1)/H \tag{3.10}$$

Furthermore, the optical cavity will have confocal parameter, b, where,

$$b \equiv 2\omega_0^2\pi/\lambda = 2(y_0^2 + \bar{y}_0^2)/H \tag{3.11}$$

and Rayleigh range,

$$z_r \equiv \omega_0^2\pi/\lambda = (y_0^2 + \bar{y}_0^2)/H \tag{3.12}$$

The far field semi angle of divergence is given by,

$$\theta = \lambda/(\pi\omega_0) = H(y_0^2 + \bar{y}_0^2)^{-1/2} = (u_0^2 + \bar{u}_0^2)^{1/2} \tag{3.13}$$

Other relationships between variables can be easily determined by constructing a yybar table. In this case, the table is constructed to determine the required Gaussian beam wavefront radii at the chosen mirror locations. Note that the yybar resonator is stabilized simply by setting the mirror radii equal to the respective (incident Gaussian beam) wavefront radii:

Table 3.2: yybar Values for an Arbitrary 2-Mirror Cavity

y	$\bar{y}$	τ	u	u	R
y_1	$\bar{y}_2$				
		L_{12}	$(y_2-y_1)/L_{12}$	$(\bar{y}_2-\bar{y}_1)/L_{12}$	
y_2	$\bar{y}_2$				$R_2 = (y_2^2+\bar{y}_2^2)/(\bar{u}_{12}\bar{y}_2+u_{12}y_2)$
		L_{21}	$(y_1-y_2)/L_{21}$	$(\bar{y}_1-\bar{y}_2)/L_{21}$	
y_1	0				$R_1 = (y_1^2+\bar{y}_1^2)/(\bar{u}_{12}\bar{y}_1+u_{12}y_1)$

From this, we can determine relationships for the mirror radii, solely in terms of the yybar variables:

$$R_2 = \frac{(y_2^2+\bar{y}_2^2)}{[\bar{y}_2(\bar{y}_2-\bar{y}_1)/L+y_2(y_2-y_1)/L]} \tag{3.14}$$

Therefore,

$$1/R_2 = 1/L - [\bar{y}_1\bar{y}_2 + y_1y_2]/\omega_2^2 L \tag{3.15}$$

And similarly,

$$1/R_1 = 1/L - [\bar{y}_1\bar{y}_2 + y_1y_2]/\omega_1^2 L \tag{3.16}$$

If we equate the common term, we obtain the useful mirror spot size relationship,

$$\omega_1^2(1/L - 1/R_1) = \omega_2^2(1/L - 1/R_2) \tag{3.17}$$

3.4   Defining the g_1, g_2 Stability Equations

The previous equation can be re-expressed as,

$$(\omega_1/\omega_2)^2 = (1 - L/R_2)/(1 - L/R_1) \equiv g_2/g_1 \tag{3.18}$$

Where g_1, g_2 are the conventional 'g-parameters' used to quantify resonator stability. In terms of the yybar variable, they are:

$$g_1 = (\bar{y}_2\bar{y}_1 + y_2y_1)/(y_1^2 + \bar{y}_1^2) \tag{3.19}$$

$$g_2 = (\bar{y}_2\bar{y}_1 + y_2y_1)/(y_2^2 + \bar{y}_2^2) \tag{3.20}$$

Although the cavity is stable (by definition) , we can use the g parameters to prove this is so. Recall the condition for resonator stability:

$$0 \leq g_1g_2 \leq 1 \tag{3.21}$$

By substitution, we have

$$0 \le [\bar{y}_1\bar{y}_2 + y_1y_2]^2 \le \omega_1^2\omega_2^2 \qquad (3.22)$$

Taking one inequality at a time, we can immediately see,

$$[\bar{y}_1\bar{y}_2 + y_1y_2]^2 \ge 0 \qquad (3.23)$$

is true for all real values of $(\bar{y}_1, y_1)$, $(\bar{y}_2, y_2)$. Taking the second inequality, we have:

$$[\bar{y}_1\bar{y}_2 + y_1y_2]^2 \le \omega_1^2\omega_2^2 \qquad (3.24)$$

which then reduces to,

$$0 \le \bar{y}_1^2 y_2^2 - 2\bar{y}_1\bar{y}_2 y_1 y_2 + \bar{y}_1\bar{y}_2 + y_1^2\bar{y}_2^2 \qquad \text{or} \qquad (\bar{y}_1 y_2 - y_1\bar{y}_2)^2 \ge 0 \qquad (3.25)$$

Therefore, the second inequality is also true for all real values of $(\bar{y}_1, y_1)$, $(\bar{y}_2, y_2)$; and thus, we have the remarkable result that <u>any two yybar coordinates form a stable resonator</u> (in accordance with our definitions).

It is a simple matter to arrive at the yybar representation for the stability 'minima'. For a simple two-mirror resonator, the condition, $g_1 g_2 = 0$ corresponds to,

$$\bar{y}_1\bar{y}_2 + y_2 y_1 = 0 \qquad (3.26)$$

or,

$$\bar{y}_2/y_2 = -y_1/\bar{y}_1 \qquad (3.27)$$

which is the confocal resonator condition, while the condition, $g_1 g_2 = 1$ corresponds to,

$$\bar{y}_1 y_2 - y_1 \bar{y}_2 = 0 \qquad (3.28)$$

or,

$$\bar{y}_2 / y_2 = \bar{y}_1 / y_1 \qquad (3.29)$$

3.5   **Graphing Common Two Mirror Cavities**

Consider the yybar diagram below:
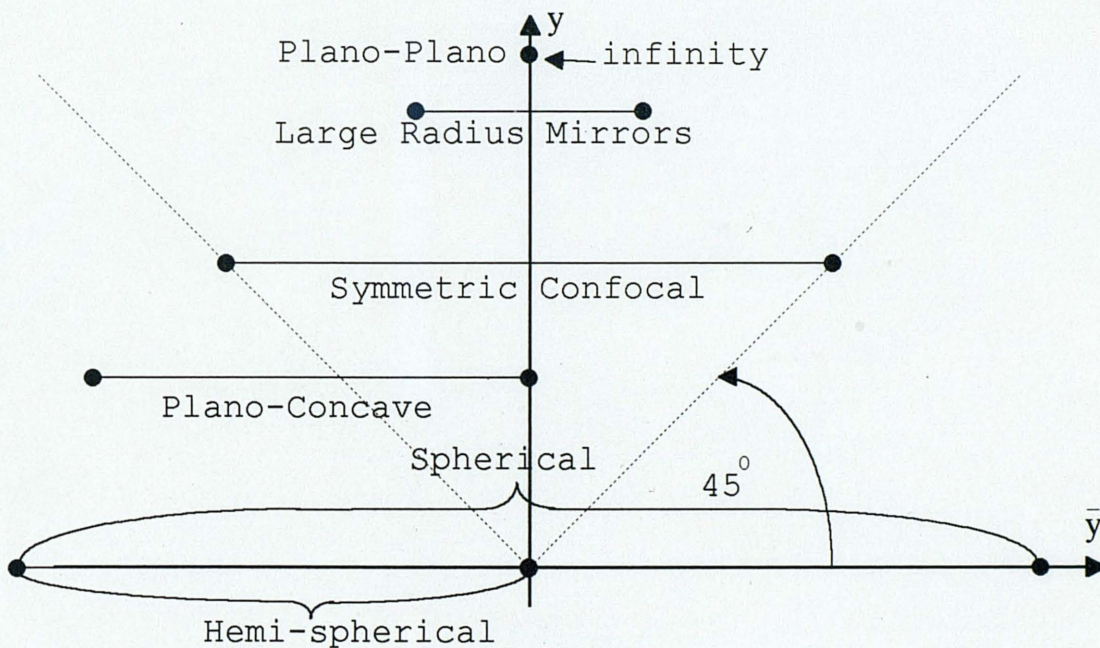

Figure 3.4: Representation of Common Two Mirror Resonator Cavities

All common (linear) optical resonators can be simply represented on the yybar plane. For

example, the confocal cavity is known to have mirror spot sizes exactly $\sqrt{2}$ times the

beam waist. Therefore, a confocal resonator is easily formed by simply defining two

points having a common y-value and intersecting the y = ± ybar lines. The plano-plano

resonator occurs for infinite beam waist. The spherical resonator approaches a zero beam

waist, and thus, in the limit, its yybar beam trace passes through the origin. Conveniently,

all extreme locations of the yybar coordinates correspond to $g_1 g_2 \rightarrow 1$, i.e., borderline

cavity stability.

3.6   Resonators with Intra-Cavity Components

It has been shown that any two yybar coordinates form a stable optical resonator,

if it is assumed that mirrors are located at these points, with radii of curvature equal to the

Gaussian wavefront. Let us now consider a generalized resonator, containing N
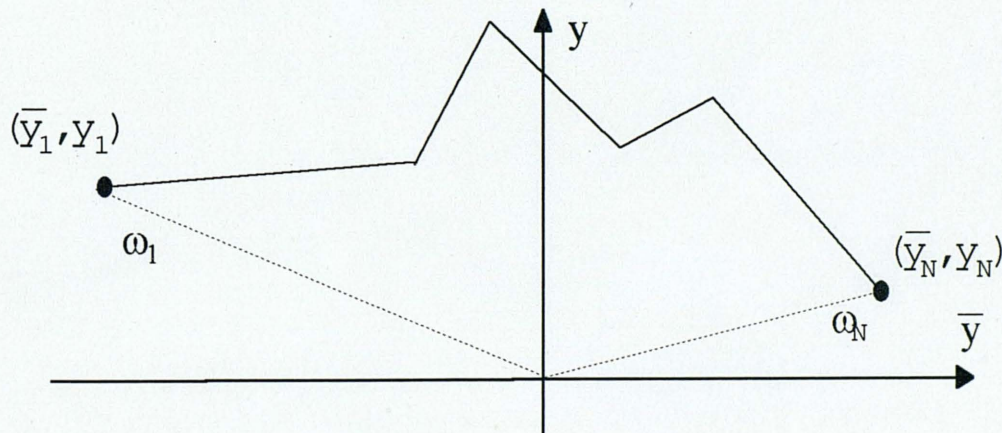
intra-cavity optical components:

Figure 3.5: Generalized N-Element yybar Resonator

By connecting each point to the origin, a series of triangular area segments are formed, representing the reduced distances traversed in traveling between the respective components. If light is traveling from left to right, the area is swept out clockwise and is considered positive. If the light is traveling from right to left, the area swept out is counterclockwise, and is considered negative, since the Lagrange invariant is also negative in this case [1.7].

Since any arbitrary pair of adjacent coordinates, $(\bar{y}_{i-1}, y_{i-1})$, $(\bar{y}_i, y_i)$ forms a stable, self-consistent, resonating path, then collectively, the sum total path must form a stable, self-consistent resonator, with mirrors located at points $(\bar{y}_1, y_1)$, $(\bar{y}_N, y_N)$. This follows from the observation that each point along the yybar resonator diagram, which represents an optical component, has <u>exactly</u> the optical power to match wavefronts to the adjacent points. In effect, the optical powers are a consequence of the yybar constraints manifesting the refraction and translation processes.

We can now generalize the method of defining an optical resonator having N optical elements (including the mirrors). The total length of the resonator is defined as,

$$L_r = \sum_{i=1}^{N} \tau_i = [\sum_{i=1}^{N}(\bar{y}_{i+1}y_i - y_{i+1}\bar{y}_i)]/H \qquad (3.30)$$

The beam size at any arbitrary location is,

$$\omega_i^2 = \bar{y}_i^2 + y_i^2 \qquad (3.31)$$

The power of the ith optical element can be determined from a yybar table:

Table 3.3: yybar Table for Determining the Power of the ith Intra-Cavity Element

y	$\bar{y}$	τ	u	u	ϕ
y_{i-1}	$\bar{y}_{i-1}$				
		$\tau_{i,i-1}$	$(y_i - y_{i-1})/\tau_{i,i-1}$	$(\bar{y}_i - \bar{y}_{i-1})/\tau_{i,i-1}$	
y_i	$\bar{y}_i$				$\phi_{i-1,i,i+1} = (u_{i-1,i} - u_{i,i+1})/y_i$
		$\tau_{i+1,i}$	$(y_{i+1} - y_i)/\tau_{i+1,i}$	$(\bar{y}_{i+1} - \bar{y}_i)/\tau_{i+1,i}$	
y_{i+1}	$\bar{y}_{i+1}$				

The radius of curvature of the wavefront, at the Nth element, is

$$R_N = (y_N^2 + \bar{y}_N^2)/(\bar{u}_{N-1,N}\bar{y}_N + u_{N-1,N}y_N) \qquad (3.32)$$

which allows a determination of one of the required mirror radii. As in the two element resonator, the other (i.e. first) mirror radius can be determined by considering the light traveling from right to left:

$$R_1 = (y_1^2 + \bar{y}_1^2)/(\bar{u}_{2,1}\bar{y}_1 + u_{2,1}y_1) \qquad (3.33)$$

In regard to the stability of these more complicated (optical system) resonators, it is useful to employ the following phase expression (although well known, this equation is conveniently derived using the yybar diagram, in chapter 4):

$$\alpha = \cos^{-1}(g_1 g_2) \qquad (3.34)$$

The extreme values of α, where $g_1 g_2 = 0$, 1, are:

$$\alpha_e = n\pi/2 \;\; ; \;\; n = \pm1, \pm2, ... \tag{3.35}$$

So that, for n odd, $g_1 g_2 = 0$, and for n even $g_1 g_2 = 1$. This result has a very simple interpretation, when viewing the yybar diagram (see figure 3.6): Whenever the end mirror coordinates are phase separated by a multiple of $\pi/2$, the resonator is at a stability minima, with odd multiples corresponding to quarter wave difference cavities, modulo four multiples corresponding to zero phase difference resonators, and odd multiples of π corresponding to $180°$ phase difference resonators. The special cases of n = 0, n = 1, n = 2 correspond to conventional plano, confocal, and spherical-type resonators, respectively. The case of zero phase difference (n = 4, 8...) corresponds to the degenerate class of cavities which have been studied in depth by Arnaud [1.3].
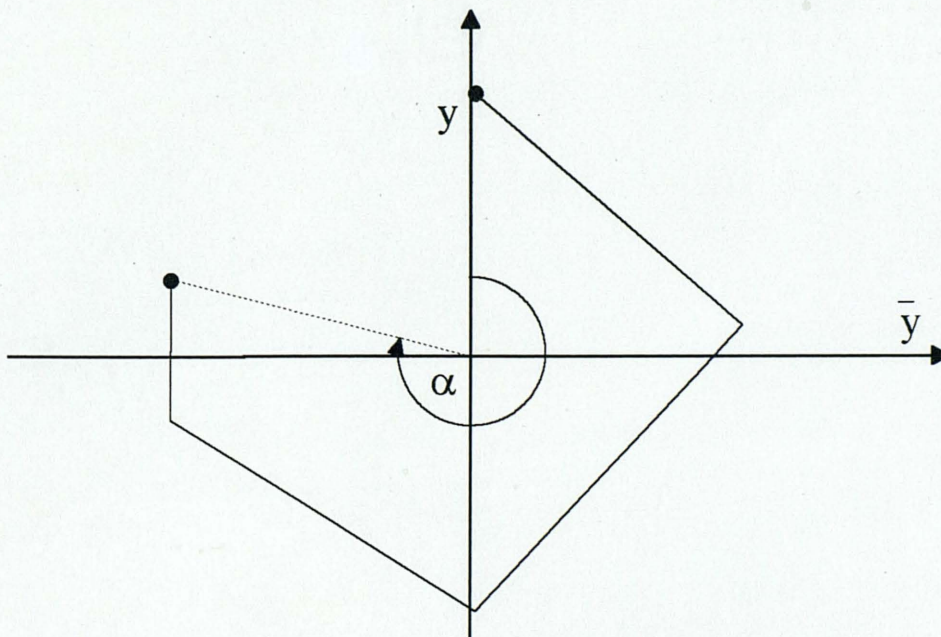

Figure 3.6: Defining the Full Resonator Phase Angle, α

CHAPTER 4

APPLICATIONS FOR THE yybar METHOD

4.1   Techniques for Applying Design Constraints

A particularly powerful advantage of the yybar diagram method is its ability to conveniently set and sustain a variety of useful beam and resonator design constraints, regardless of how complicated the internal optical system may be. In contrast to conventional resonator design procedures, the yybar method allows mirror radii and internal lens focal power to 'float' in value, while retaining what may be more important constraints. For example, one may wish to fix the resonator length and stability characteristic, while adding any number of intra-cavity components for beam manipulation. In another example case, we may wish to set the mirror spot sizes and waist size, while adjusting imaging properties and lens power. After the system design is basically established, the mirror radii and lens powers can be chosen appropriately.

The yybar method also accommodates the more conventional design constraint method of first choosing the mirror and lens powers and their respective spacing, and then determining the resonator stability and beam properties via the yybar coordinates. However, with the yybar information, we are then equipped with a substantial byproduct: a complete resonator ray trace is derived, simply by plotting the yybar diagram. This topic is discussed later in the section entitled, "Generating the yybar Diagram, Given the

ABCD Matrices. For the current discussion, let's examine three important and useful techniques of setting yybar resonator constraints: Using normalization, locking the resonator phase angle, and setting the magnitude of the beam 'vector'.

The advantage gained by normalizing the yybar set has been discussed by López-López. Here, we apply the normalization method in order to constrain the optical resonator length to a chosen value, regardless of the number of intra-cavity components. We define a normalization length,

$$\mathbb{L} = \left[\frac{1}{L}\left[\sum_{i=1}^{N}(\overline{y}_{i+1}y_i - y_{i+1}\overline{y}_i)\right]\right]^{1/2} \tag{4.1}$$

By dividing the yybar set by this length, i.e.,

$$\overline{\mathbb{y}} = \overline{y}/\mathbb{L} \qquad \text{and} \qquad \mathbb{y} = y/\mathbb{L} \tag{4.2}$$

and then using the reduced set, $\{\mathbb{y}, \overline{\mathbb{y}}\}$, the cavity length, L, is always preserved.

The second constraint technique of locking the phase angle, has the advantage of securing the stability characteristic of the resonator, while adding any number of intra-cavity elements or changing the length of the resonator. The prescription for using this strategy is as follows:

(1)   Choose the desired phase angle or stability characteristic.

(2)   Sketch the yybar diagram for a resonator which subtends the required
        phase angle with respect to the origin, and which achieves the desired
        beam path and image properties.

(3)   Normalize all yybar coordinates by the desired resonator length.

(4)   Fill in a yybar table with the normalized coordinates, and compute the required mirror and lens powers.

(5)   Adjust the length, if required to obtain the desired beam dimensions and/or commercially available mirror radii, and iterate, if necessary.

The third and final constraint technique discussed here is the most basic, and involves the setting of the beam vector magnitude. This particular design tool represents a very practical capability, since one may choose, at the very outset of selecting a resonator design, to simply choose the desired beam size at any desired location in the resonator. A prescription for using this constraint method is as follows:

(1)   Choose the desired beam spot size for the first mirror.

(2)   Determine starting yybar coordinates by using the beam vector magnitude relation, $\omega_1 = \sqrt{y_1^2 + \bar{y}_1^2}$

(3)   Plot the coordinate on a yybar diagram, and then choose any other desired points in a clockwise manner, ending with the second end mirror. Realize that the chosen points determine the desired beam size via the beam vector magnitude relation. Use the area swept out by the beam vector to determine the reduced distance between coordinates.

(4)   Choose the location of the beam waists by setting the yybar trace perpendicular to the beam vector.

(5)   Determine the required resonator length and the lens and mirror focal powers by filling out a yybar table.

4.2   Obtaining Other Important Beam Equations

The yybar diagram and variables also allow new methods of deriving important resonator beam relationships. The following two examples elegantly demonstrate the simplicity the method offers. The reader is encouraged to find and compare conventional resonator algebra methods of deriving these key equations.

In the first example, we will derive the general mirror spot size equations. Consider the area of the parallelogram, formed by the yybar origin and any two (non-zero) coordinates (see Figure 4.1):

$$\text{area} = \omega_1 \omega_2 \sin\alpha = \begin{vmatrix} y_1 & \bar{y}_1 \\ y_2 & \bar{y}_2 \end{vmatrix} = L_{12}H \tag{4.3}$$

which is simply the 'beam vector' cross-product (the beam vector is defined in the section on Phase Diagrams). This gives,

$$\omega_1 \omega_2 = L_{12}H/(1 - \cos^2\alpha)^{1/2} \tag{4.4}$$

If we multiply this equation by the relation, $\omega_1/\omega_2 = (g_2/g_1)^{1/2}$, we obtain,

$$\omega_1^2 = (g_2/g_1)^{1/2}L_{12}H/(1 - \cos^2\alpha)^{1/2} = L_{12}H(g_2/g_1)]^{1/2}/(1 - g_1 g_2)^{1/2} \tag{4.5}$$

or, $$\omega_1^2 = L_{12}(\lambda/\pi)[g_2/(g_1(1 - g_1 g_2))]^{1/2} \tag{4.6}$$

and similarly,

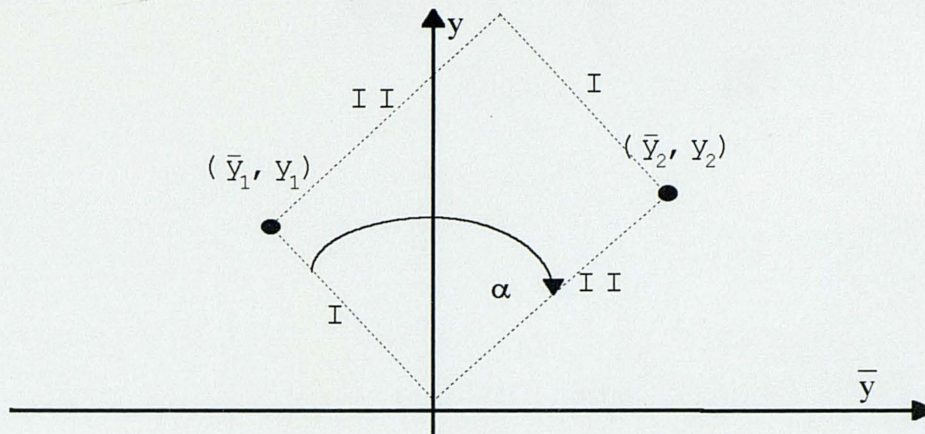$$\omega_2^2 = L_{12}(\lambda/\pi)[g_1/(g_2(1 - g_1 g_2))]^{1/2} \tag{4.7}$$

Figure 4.1: yybar Representation of the Beam Vector Cross-Product

In the second example, we will prove the important phase relationship,

$$\alpha = \cos^{-1}(g_1 g_2)^{1/2} \tag{3.33}$$

<u>Proof</u>:

Angle between two lines passing through the origin is,

$$\tan \alpha = (s_1 - s_2)/(1 + s_1 s_2) \tag{4.8}$$

where s_1 and s_2 are the line slopes. Therefore,

$$\tan \alpha = \frac{(\frac{y_1}{\bar{y}_1} - \frac{y_2}{\bar{y}_2})}{(1 + \frac{y_1 y_2}{\bar{y}_1 \bar{y}_2})} = \frac{\bar{y}_2 y_1 - y_2 \bar{y}_1}{\bar{y}_1 \bar{y}_2 - y_1 y_2} \tag{4.9}$$

The numerator was just shown to be $\omega_1 \omega_2 \sin \alpha$ in the previous example, while the

denominator is just $\omega_1^2 g_1$. So we have,

$$\tan\alpha = \frac{\omega_1\omega_2\sin\alpha}{\omega_1^2 g_1} = \left(\frac{\omega_2}{\omega_1}\right)\frac{\sin\alpha}{g_1} \tag{4.10}$$

giving,

$$1/\cos\alpha = \pm\left(\frac{g_1}{g_2}\right)^{1/2}\left(\frac{1}{g_1}\right) \tag{4.11}$$

or,

$$\alpha = \cos^{-1}(g_1 g_2)^{1/2}$$

4.3   Defining Real Beams with the M^2 Parameter

Consider a modified, but untruncated beam such that [4.1],

$$1/q = 1/R - iM^2\lambda/\pi\omega^2 \tag{4.12}$$

The M^2 parameter in this equation represents a modification to the gaussian beam to account for so-called 'real laser beam' qualities, such as multi-mode effects. Siegman defines $M^2 = 4\pi\sigma_0\sigma_s$, where σ_0 and σ_s are the beam's minimal spatial variance and spatial frequency variance, respectively [2.2-2.4].

By comparing this modified definition for the complex q parameter to the general equations, the value of relating the yybar variables to a general complex radius of curvature is again made evident. We can immediately see that the M^2 parameter simply represents a scale factor for the TEM_{00} Lagrange Invariant:

$$H_M = M^2\lambda/\pi = M^2 H \tag{4.13}$$

Equivalently, we can determine the modified yybar and uubar parameters in terms of their original values. Since,

$$M^2H = MyM\bar{u} - M\bar{y}Mu \qquad (4.14)$$

then, the transformation equations for representing generalized Gaussian beams become,

$$y_M = My \qquad\qquad u_M = Mu \qquad (4.15)$$

$$\bar{y}_M = M\bar{y} \qquad\qquad \bar{u}_M = M\bar{u} \qquad (4.16)$$

Therefore,

$$\omega_M = M(\bar{y}^2 + y^2)^{1/2} = M\omega \qquad (4.17)$$

and,

$$\theta_M/2 = M^2\lambda/(\pi\omega_0) = H_M(y_0^2 + \bar{y}_0^2)^{-1/2} = M^2H(y_0^2 + \bar{y}_0^2)^{-1/2} \qquad (4.18)$$

These relations conform exactly with Siegman's real beam definitions. Although the optical invariant is in general different for our new beam, we can conveniently represent it as a scaled version of its intrinsic ($M^2 = 1$) mode. By plotting both beam modes on the yybar plane (Figure 4.2), we obtain a very simple technique for characterizing their differences. Since most optical resonators have inherent non-gaussian, aberration and diffraction properties, the M^2 version of the Lagrange Invariant is extremely useful. For yybar purposes, we can also assign a special value to

M^2 for conveniently scaling the diagram to suit wavelength effects, as well. If we let

$M_\lambda^2 = \lambda_2/\lambda_1$,where $\lambda_2 \geq \lambda_1$, and λ_1 represents our base Invariant wavelength, then we

can effectively achromatize the yybar system in the manner described by Kessler and

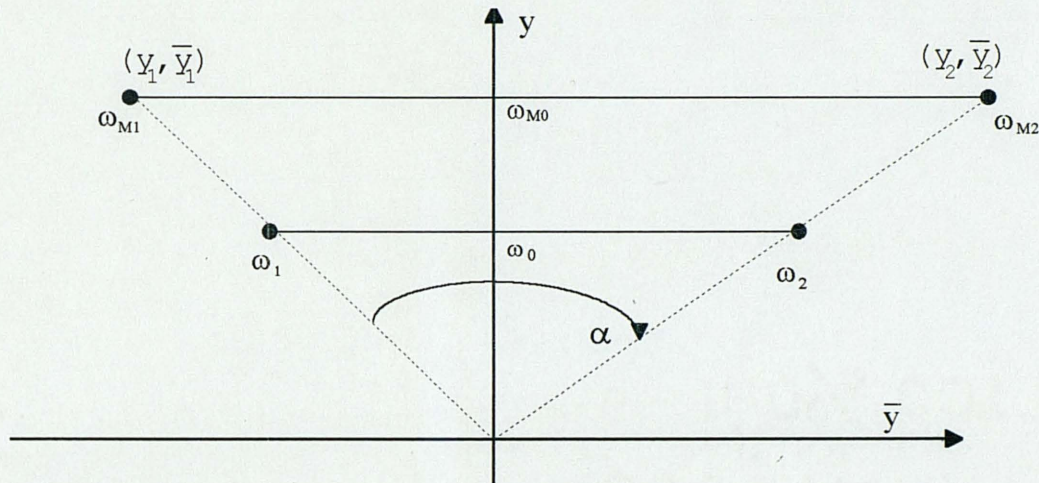Shack, enabling us to describe properly scaled multi-wavelength resonators.

Figure 4.2: Graphical Definition of the M^2 Beam Parameter on the yybar Diagram

4.4   Using the yybar Diagram as a Phase Diagram

The normalized gaussian beam solution to the wave equation is [2.1]:

$$\Psi(z) = \left(\frac{2}{\pi}\right)^{1/2} \left(\frac{1}{\omega(z)}\right) \exp(-j\phi(z))\exp[-jkr^2/2q(z)] \qquad (4.19)$$

where $\phi(z)$ is the 'Guoy' phase shift measured with respect to $z = 0$. Recalling,

$$\tan(\phi) = \lambda z/\pi\omega_0^2 \qquad (4.20)$$

We then have by substitution,

$$\tan(\phi) = z(u_{0z}^2 + \bar{u}_{0z}^2)^{1/2}/H \qquad (4.21)$$

or,

$$\tan(\phi) = (y_z u_{0z} + \bar{y}_z \bar{u}_{0z})/(y_z \bar{u}_{0z} - \bar{y}_z u_{0z}) \qquad (4.22)$$

Consider the case $u_{0z} = 0$. Let this phase angle be ϕ_{0z}:

$$\tan \phi_{0z} = \bar{y}_z/y_z \qquad (4.23)$$

Therefore,

$$\mathbf{Y}^* = \omega(y/\omega - j\bar{y}/\omega) = \omega \exp(-j\phi_{0z}) \qquad (4.24)$$

and so,

$$1/\mathbf{Y}^* = (1/\omega)\exp(-j\phi_{0z}) \qquad (4.25)$$

The definition of the phase angle in this form was previously prescribed by Arnaud. In terms of the yybar variables, the gaussian solution becomes,

$$\psi(z) = \mathbf{Y}^* \exp(-jk\dot{\mathbf{Y}}r^2/2\mathbf{Y}) \qquad (4.26)$$

so that ,

$$\Psi(z) = \psi(z) \sqrt{\frac{2}{\pi}} \exp(-jkz) \qquad (4.27)$$

The yybar diagram allows an extremely convenient interpretation of the Guoy phase shift (see Figure 4.3) when the starting reference point (in this case the first mirror) is located along the y axis (i.e. ybar=0), and for this special case of $u_{0z} = 0$: It is simply the yybar polar angle, measured with respect to the y-axis. Note that a simple rotation of the yybar system can transform the position of the beam waist so that $u_o = 0$. (As was mentioned in Chapter 3, a rotation effectively defines an alternate, but equivalent, pair of paraxial rays.)
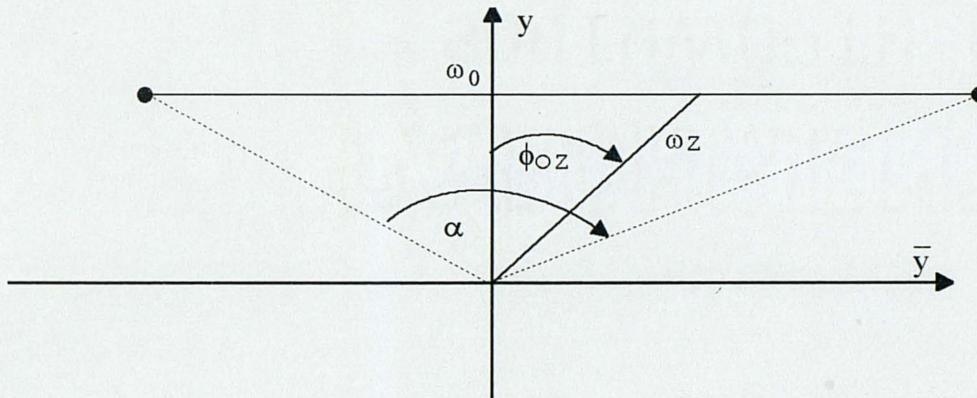

Figure 4.3: Guoy Phase Shift Definition on a yybar Diagram

Another convenient and useful method of defining the phase of a resonator is as follows. As before, consider an optical resonator with mirrors defined by two arbitrary points on the yybar diagram; this allows u_{0z} to be any finite value. Let's also define the more general polar angle, θ:

$$\tan\theta(z_i) = \bar{y}_i/y_i \tag{4.28}$$

which defines the location and magnitude of the beam vector, $\vec{\omega}_i$ (see Figure 4.4). By geometry, the relative phase shift along the complete cavity is:

$$\phi(z_1) - \phi(z_2) = \theta(z_1) - \theta(z_2) = \alpha \qquad (4.29)$$

This yields the useful relationship,

$$g_1 g_2 = \left| \cos[\tan^{-1}(\bar{y}_2/y_2) - \tan^{-1}(\bar{y}_1/y_1)] \right| \qquad (4.30)$$

Finally, if the first mirror is specially chosen such that $\bar{y}_1 = 0$, then we have simply,

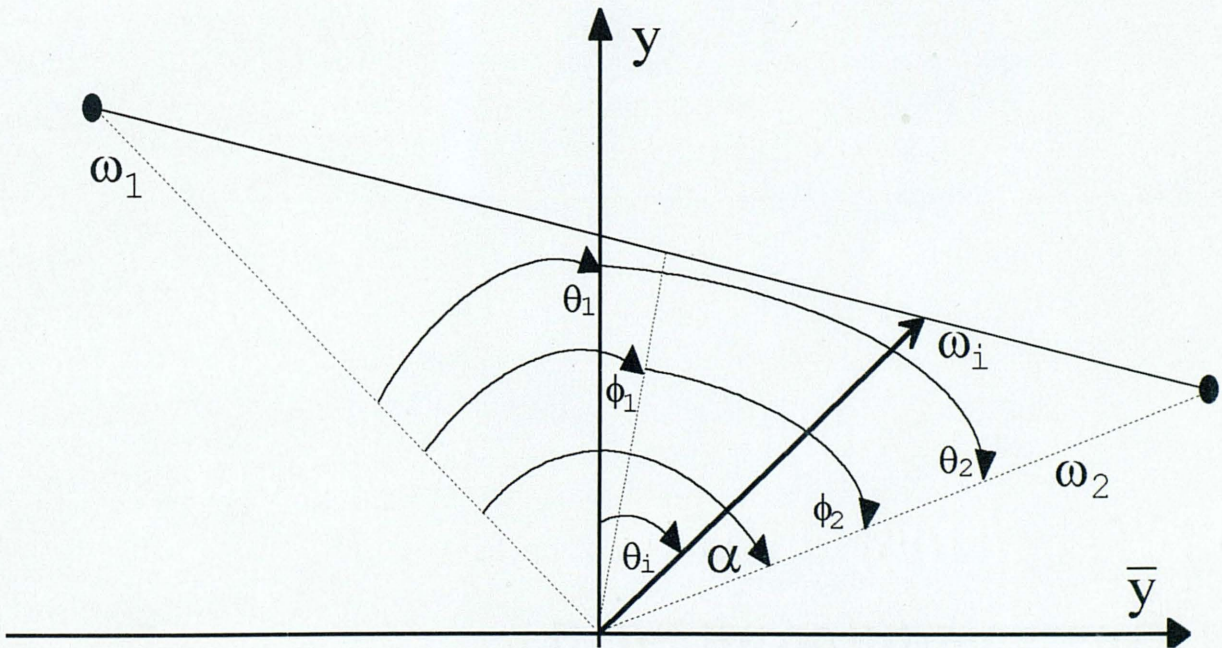$$g_1 g_2 = y_2/(y_2^2 + \bar{y}_2^2)^{1/2} \qquad (4.31)$$

Figure 4.4: Diagram Showing the Beam Vector Geometry

4.5   Determining Resonant Frequencies

For a resonant standing wave cavity, the total round trip phase difference is an integer multiple of 2π:

$$2L/H - [\tan^{-1}(\bar{y}_2/y_2) - \tan^{-1}(\bar{y}_1/y_1)] = 2n\pi \qquad (4.32)$$

The resonant wavelengths are:

$$\lambda_r = \frac{2\pi L}{2\pi n + [\tan^{-1}(\bar{y}_2/y_2) - \tan^{-1}(\bar{y}_1/y_1)]} \qquad (4.33)$$

and the resonant frequencies are:

$$\nu_r = [2\pi n + \tan^{-1}(\bar{y}_2/y_2) - \tan^{-1}(\bar{y}_1/y_1)](c/2\pi L) \qquad (4.34)$$

The Optical Resonator Lagrange Invariant, $H = \lambda_r/2\pi$, is thus shown to actually have multiple, discrete values.

4.6   Generating the yybar Diagram, Given the ABCD Matrices

Consider the general case of a pre-defined optical resonator with two end mirrors and an internal lens system. In this case, mirror radii, lens focal lengths, and all respective spacing are already specified. A method is proposed here to determine the yybar system representation and effectively obtain a complete resonator ray trace, using the specified radii constraints:

(1)   Determine the overall optical system ray coefficients, A,B,C, and D.

(2)   Compute the g_1, g_2 values using the relations Kogelnik derived in 1965:

$$g_1 = (A - B/R_1) \qquad\qquad g_2 = (D - B/R_2) \qquad\qquad (4.35)$$

(3)   Determine the starting y coordinate for the first mirror by computing the mirror spot size. Set the corresponding ybar coordinate to zero.

(4)   Use the relations, u=y/R, and ubar=H/y, to determine the starting paraxial angles.

(5)   Compute the y and ybar coordinates for each intra-cavity component by using the standard ABCD transfer relations.

4.7   <u>Synthesizing Resonators</u>

"It is apparent that the yybar diagram is useful in the analysis of given systems because of the ease which one can determine all the first-order characteristics... however, the greatest value is in the synthesis rather than analysis." -- Roland Shack [1.11].

This observation is generally applicable to all yybar optical systems, but it is especially appropriate for optical resonators where dynamic effects (such as thermal lensing) can be important and where the constraints of cavity length and wavefront curvature apply. In all cases, the system is completely deduced, <u>automatically</u>, as soon as the yybar diagram is established. Furthermore, this strategic graphical device can immediately identify allowable changes in the system. Chosen constraints can be applied, while varying other selected parameters; and the resultant component optics can be synthesized from these constraints.

Several examples should serve to demonstrate the power of yybar synthesis:

Consider an optical resonator with two arbitrary internal lenses and two flat mirrors,

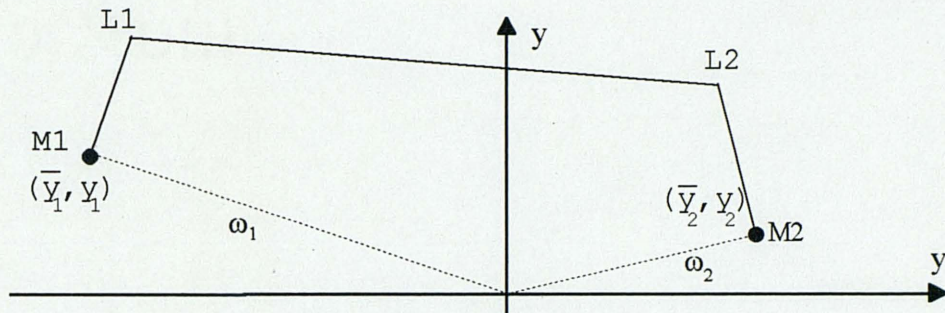having the yybar diagram pictured below:

Figure 4.5: Flat-Flat Resonator with Two Intra-cavity Lenses

According to the yybar principles, the total length of the resonator is proportional

to the enclosed area of the pentagon. Consequently, we can form an alternative resonator,

if we choose M1, M2 and length as example constraints, and vary the L1, L2 focal lengths

and spacing.

One possible configuration is a telescopic conjugating resonator, with the beam

waists imaged on each other. It is a simple matter to compose such a configuration on a
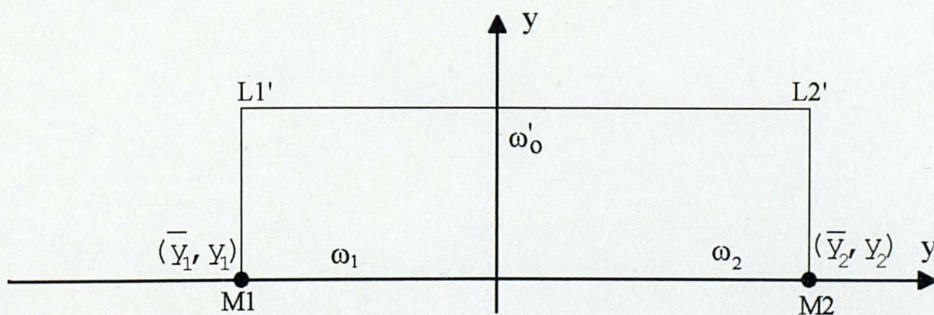
yybar diagram:

Figure 4.6: Synthesized 'Afocal' Flat-Flat Resonator

In this case, we have also chosen to maintain the same beam spot sizes at the flat

mirrors. Note that the area of the enclosed rectangle is the same as the pentagon area.

Therefore, the value of $\omega_0^{'}$ can be determined. The remaining quantities are readily

evaluated [1.6]. The distance between the lenses is $f_1' + f_2'$. The distance from the mirror,

M1, to the first lens is f_1' . Similarly, the distance from the second lens to the mirror, M2,

is f_2' . The magnification, $m = -\omega_2/\omega_1 = -f_2'/f_1'$. The focal lengths of the lenses are then

related to the cavity length by $L = 2(f_1' + f_2') = 2f_1'(1 + \omega_2/\omega_1)$.

As a second example, assume we are given a simple two-mirror cavity. Depicted
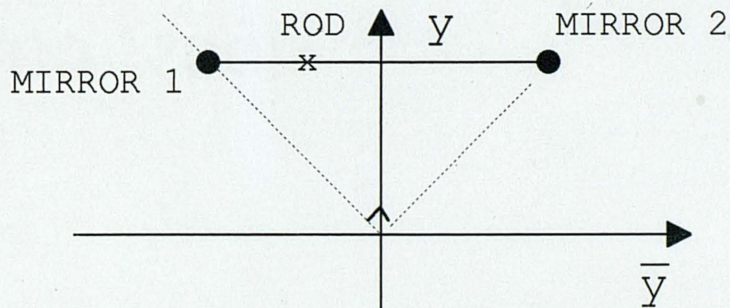
on the yybar plans, the diagram is:

Figure 4.7: Initial Confocal Laser Resonator

Our problem is to modify the cavity to allow a tight intra-cavity focus, but maintain the

same beam curvature at M1, and the same beam size at M1 and M2. One approach is to

form an intra-cavity relay arrangement (reference LASERSCOPE Patent #5,025,446).

The yybar diagram can be easily employed to demonstrate the principle utilized in this type

of design. Referring to the figure below, we can simply 'wrap' a cycle around the origin, assuming cavity length is not a constraint:
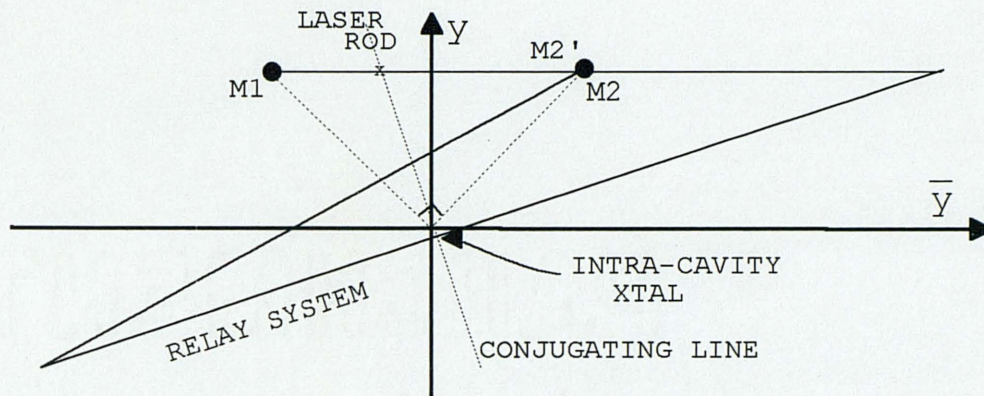

Figure 4.8: Synthesized Conjugating (Confocal) Intra-cavity Doubling Resonator

Here, a two-mirror arrangement is used to relay the mirror, M2 to M2'. The beam size at the two mirrors is maintained, while the curvature of M2 is not. The cavity $g_1 g_2$ parameters are kept constant.

The most noteworthy feature of the new design is the tight intra-cavity focus, allowing for efficient frequency conversion if a non-linear crystal were to be placed at this location. In addition, the crystal location can be made conjugate to where the laser rod is possibly situated. Such an arrangement is reported to minimize thermal lensing effects in the frequency doubling process. It is interesting to note that a thorough reading of the cited patent for a design of this type will not yield nearly as much insight into the system principles as has this simple process of synthesizing an equivalent compound yybar cavity, from the given constraints.

SUMMARY AND RECOMMENDATIONS

5.1 Summarizing the New yybar Resonator Design Method

The Gaussian beam resonator formalism using the yybar method has been

shown to:

(1)   present a novel and useful method for designing automatically stable resonators.

(2)   suggest insight into the origin of the ABCD law for the conventional complex q parameter.

(3)   provide an elegant, simple and effective method for complete Gaussian beam resonator ray tracing, given the conventional ABCD ray coefficients.

(4)   contribute some new and simpler ways for obtaining important resonator beam equations.

(5)   offer a potentially complete and powerful tool for designing, optimizing, analyzing, and synthesizing complicated multi-element resonator designs.

(6)   conveniently describe resonator phase properties and M^2 beams.

5.2 Recommendations for Further Development to the Theory

(1)   Generate computer software program to implement the yybar resonator formalism

(2)   Compare software results to other commercial software (apply test cases and debug, if necessary).

(3)   Demonstrate the software for at least three practical resonator problems:

> (a) Thermal lensing
> (b) Astigmatic effect in ' z-fold ' cavity
> (c) Mode matching
> (d) Laser system integration

(4)   Extend the model to account for important third order aberration effects.

(5)   Implement 'complex' components (Gaussian mirrors, Kerr medium, gain guiding)

(6)   Define unstable and ring cavities

(7)   Add additional information to the yybar diagram (intensity, back-reflections)

(8)   Study mis-alignment effects

REFERENCES

[1.1]   R. R. Shannon, "The Changing Nature of Lens Design," Optics and Photonics News, July, p. 38 (1993).

[1.2]   H. Kogelnik, "Imaging of Optical Modes--Resonators with Internal Lenses," Bell Syst. Tech J.**44** , pp. 455-494 (1965); H. Kogelnik, "On the Propagation of Gaussian Beams of Light Through Lenslike Media Including those with a Loss or Gain Variation," Appl. Opt. **4**, pp. 1562-1569 (1965); H. Kogelnik and T. Li, "Laser Beams and Resonators," Proc. of IEEE , vol. **54**, pp. 1312-1329 (1966); H. Kogelnik, "Propagation of Laser Beams," Applied Optics and Optical Engineering, vol. **VII**, pp. 155-190, The Academic Press (1979).

[1.3]   J. A. Arnaud, "Degenerate Optical Cavities," Appl. Opt. **8**, pp. 189-195 (1969); J. A. Arnaud, "Degenerate Optical Cavities. II: Effect of Misalignments," Appl. Opt. **8**, pp. 1909-1917 (1969).

[1.4]   J. Arnaud, "Representation of Gaussian Beams by Complex Rays," Appl. Opt. **24**, pp. 538-543 (1985).

[1.5]   D. Kessler and R. V. Shack, "First-Order Design of Laser Systems with the $y\bar{y}$ Diagram," OSA Annual Meeting, TuF2 (1984).

[1.6]   D. Kessler and R. V. Shack, "The $y\bar{y}$ Diagram, a Powerful Optical Design Method for Laser Systems," Appl. Opt. **31**, pp. 2692-2707 (1992).

[1.7]   E. Delano, "First-Order Design and the $y, \bar{y}$ Diagram," Appl. Opt. **2**, pp.1251-1256 (1963).

[1.8]   R. J. Pegis, T. P. Vogl, A. K. Rigler, and R. Walters, "Semiautomatic Generation of Optical Prototypes," Appl. Opt**. 6**, pp. 969-972 (1967).

[1.9]   F. J. López-López, "Normalization of the Delano Diagram," Appl. Opt. **9**, pp. 2485-2488, (1970).

[1.10] F. J. López-López, "Analytical Aspects of the $y\bar{y}$ Diagram," Proc. of SPIE, vol. **39**, pp. 151-159 (1973).

[1.11] R. V. Shack, "Analytic System Design with Pencil and Ruler--The Advantages of the yȳ diagram," Proc. of SPIE, vol. **39**, pp. 127-140 (1973).

[1.12] W. Besenmatter, "Designing Zoom Lenses Aided by the Delano Diagram," SPIE, vol. **237**, pp. 242-250 (1980).

[1.13] M. E. Harrington, R. P. Loce, and J. Rogers, "Use of the yȳ Diagram in GRIN Rod Design, " Appl. Opt. **27**, pp. 459-464 (1988).

[1.14] J. Rogers, M. E. Harrington, and R. P. Loce, "The yȳ Diagram for Radial Gradient Systems," Appl. Opt. **27**, pp. 452-458.

[1.15] P. Trotta, "The Optical Invariant," Optics and Photonics News, July, p. 56 (1994). P. Trotta, "The Optical Invariant II," Optics and Photonics News, September, pp. 34-35 (1994).

[1.16] R. Herloski, S. Marshall, and R. Antos, "Gaussian Beam ray-equivalent Modeling and Optical Design," Appl. Opt. **22**, pp. 1168-1174 (1983).

[1.17] Ealing Optics Catalog, pp. 178-179 (1995)

[2.1]   A. Siegman, *Lasers* (Mill Valley, California: University Science Books, 1986).

[2.2]   A. E. Siegman, "New Developments in Laser Resonators," in *Laser Resonators*, D. A. Holmes, ed., Proc. SPIE, vol. **1224**, pp. 2-14 (1990).

[2.3]   A. E. Siegman, "Defining the Effective Radius of Curvature for a Nonideal Optical Beam," IEEE Journal of Quantum Electronics, vol. **27**, pp. 1146-1148 (1991).

[2.4]   A. E. Siegman and S. W. Townsend, "Output Beam Propagation and Beam Quality from a Multimode Stable-Cavity Laser," IEEE Journal of Quantum Electronics, vol. **29**, pp. 1212-1217 (1993).

[2.5]   A. Yariv, *Optical Electronics* (New York: Holt, Rinehart & Winston, 1985).

[2.6]   J. T. Verdeyen, *Laser Electronics* (New Jersey: Prentice Hall, 1989).

[4.1]   P. A. Bélanger, "Beam Propagation and the ABCD Ray Matrices," Optics Letters, vol . **16**, pp. 196-198 (1991).